Comparison of Variability in Results of Acoustic Tomographs in Pedunculate Oak (*Quercus robur* L.)

Valentino Cristini,[a] Jan Tippner,[a] Barbora Vojáčková,[a] and Vinko Paulić [b]

Tree acoustic tomography is a widely used device-supported method for tree stability assessment. In this work, the results of the three most commonly used devices for acoustic tomography of standing trees (ARBOTOM®, ArborSonic®, and PiCUS®) were compared on selected individuals of sessile oak in Brno, Czech Republic. According to the statistical analysis, there was a significant difference between values measured by the PiCUS® acoustic tomograph and those measured by both the ARBOTOM and ArborSonic® acoustic tomographs. Based on the measured data, velocities measured by PiCUS® were considerably lower than those recorded by the other acoustic tomographs (ARBOTOM® and ARBORSONIC®). Measured radial and tangential velocities differed from each other. In data obtained from the defective cross-sections, this difference was attenuated. Image reconstructions (tomograms) from the acoustic tomographs differed from each other. Complex shapes of defects in standing trees can significantly influence acoustic tomography results. According to the statistical analysis, there was no significant relationship between sound velocity and density, while there was a relatively strong positive correlation between sound velocity and moisture content.

Keywords: Acoustic tomograph; Sound velocity; Density; Moisture content; Trees

Contact information: a: Mendel University in Brno, Faculty of Forestry and Wood Science, Department of Wood Science and Technology, Zemědelská 1665/1, 613 00 Brno, Czech Republic; b: University of Zagreb, Faculty of Forestry, Department of Ecology and Silviculture, Svetošimunska 25, 10 00 Zagreb, Croatia;
** Corresponding author: valentino.cristini@gmail.com*

INTRODUCTION

One of the main issues of tree care in an urban environment is ensuring public safety. With trees in streets and parks, the risk of damage to property and public health is significantly higher than in forests; therefore, trees growing on such sites need to be monitored (Sterken 2005). Trees outside the forest environment are more exposed to various negative abiotic and biotic factors (*e.g.*, hydric stress, negative anthropological interventions) (Ordóñez-Barona *et al.* 2018), which in some cases affect the tree in a destructive and irreversible manner.

Some damage or rot adversely affecting the stability of trees is not detectable by visual assessment. Consequently, the use of device-supported methods is necessary in such cases (Wang *et al.* 2001; Wen *et al.* 2016). Different techniques are based on acoustics, where the propagation velocity of stress waves is measured among the radial or longitudinal axis of the stem (Arciniegas *et al.* 2014). According to their low invasiveness, acoustic methods are regarded as non-destructive and therefore many times repeatable on the same specimen without creating relevant damage to assessed stem or branch (Brashaw *et al.* 2009). The decrease in measured velocity may correspond to a longer path of the measured signal due to the presence of internal defects or degraded wood (Wang *et al.*

2004). These methods were developed afterwards to create acoustic tomography (AT), which detects defects in radial cross-sections of a stem by the velocity of stress wave propagation (Liang *et al.* 2008; Wang 2013). Compared to conventional acoustic testing techniques, AT can create a spatial estimation of the defect in two or three dimensions. Beside the matrix of measured velocities among all sensors, the main result consists of a computed image reconstruction, which shows the theoretical integrity of wood on a cross-section at the chosen height (Maurer *et al.* 2006; Du *et al.* 2018). AT was first used for inspections of wooden poles (Tomikawa *et al.* 1986). Later, it was applied in non-destructive tree stability assessment (Wang *et al.* 2004). By comparing visual assessments of decay in cross-sections with tomography results, Gilbert and Smiley (2004) demonstrated the ability of AT to determine the degradation level of wood in oak (*Quercus alba* L.) and hickory (*Carya* spp.). The average accuracy of samples with wood degradation detected by the device was approximately 89%. Rioux (2004) tested 10 white oaks and three hickory trees and found a 5% difference between AT and actual states of decay on average. In addition to identification of decay, Alves *et al.* (2015) showed the importance of AT in determining elastic constants of Muiracatiara Brazilian wood (*Astronium lecointei*). Recently, different image reconstruction methods have been developed and presented (Espinosa *et al.* 2017; Du *et al.* 2018). According to the reliable representation of cavities and degraded wood, AT can be used to predict the loss of load-bearing capacity for trees with internal defects (Burcham *et al.* 2019).

However, different factors influence the behaviour of stress wave propagation due to the heterogeneity of wood properties in standing trees (Alméras *et al.* 2005). For example, the wave propagation velocity is greater in the radial direction than in the tangential one (Palma *et al.* 2018). Another factor is moisture content. An increase in moisture content in wood causes the velocity of sound transmission to decrease (Sandoz 1989; Unterwieser and Schickhofer 2011; Montero *et al.* 2015); however, this clearly applies to the longitudinal direction only. Taking into account that the speed of sound in water at room temperature is approximately 1500 m/s (Kumar *et al.* 2016) and the speed of sound wave propagation perpendicular to the fibres (in the radial direction) is in the range of 1000 to 2000 m/s (Divos and Divos 2005), the presence of free water in wood may significantly influence the propagation speed of acoustic waves.

Another discussed factor is wood density. Baar *et al.* (2012) and Ilic (2003) state that the sound propagation is not significantly dependent on wood density. In contrast, de Oliveira and Sales (2006) argue that as the density increases, the speed of sound tends to increase. Bucur and Chivers (1991) state that with increasing density, the speed of stress waves decreases.

The acoustic tomographs used the most in commercial enterprises are PiCUS® (Argus Electronic gmbh, Rostock, Germany), ARBOTOM® (Rinntech-Metriwerk GmbH & Co. KG, Heidelberg, Germany), and ArborSonic® (Fakopp Enterprise Bt., Agfalva, Hungary). Siegert (2013) compared image reconstructions (tomograms) of the three tomographs and eliminated variability by using the same position of measurement points. The author found that the divergence in results among tomographs is caused by different settings of tools and related software. Schubert (2007) and Arciniegas (2014) compared components of measurement systems among a range of another devices based on the sound transmission.

Table 1. Main Differences between Compared Acoustic Tomographs (Arciniegas *et al.* 2014)

Parameters / Device	Excitation	Sensor	Picker	Inversion	Rays	Material
PiCUS®	IH	Accelerometers	Threshold	Modified FBP	Straight	Isotropic
ARBOTOM®	IH	Accelerometers	NS	NS	NS	NS
ArborSonic®	H	Accelerometers	Threshold	NS	NS	NS

IH instrumented hammer, *H* hammer, *FBP* filtered back projection, *NS* not specified.

However, none of these publications discuss the difference in measured stress wave velocities between the three commonly used tomographs (PiCUS®, ARBOTOM®, and ArborSonic®). This study evaluated the consistency of these tomographs in terms of stress waves propagation velocity and image reconstruction. The correlation of velocity with density and moisture content is also considered.

EXPERIMENTAL

Three pedunculate oaks situated in Brno-Sobešice (Czech Republic) with a diameter at breast height range of 23 to 29 cm were measured. Two of them showed symptoms of decay (enlarged butt end, mechanical damage) just above the ground level. The trees were measured with three acoustic tomographs (PiCUS®, ARBOTOM® and ArborSonic®) at the same height. A 10-cm-thick disk at each tested height was removed and photographed. To validate field testing, discs from tree no. 1 were sampled for laboratory measurement. To prevent the wood from drying during transportation to the laboratory, samples were sealed in plastic bags.

Acoustic Tomography Measurement

Measurements was performed in March of 2019, and the average daily temperature was 12 °C. The first three trees were measured at two levels and the last one at one level.

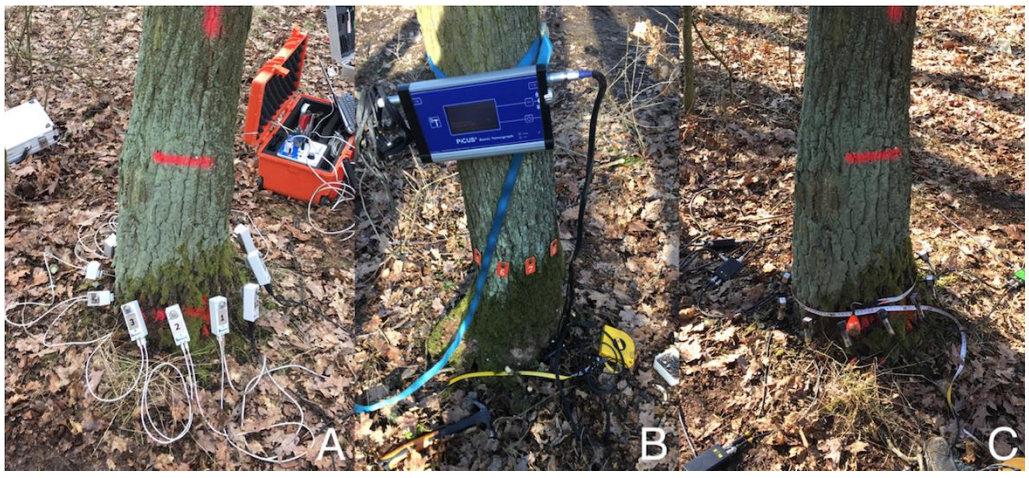

Fig. 1. Acoustic tomography set-up: A - ARBOTOM®, B - PiCUS®, C - ArborSonic®

The measurement heights ranged between 15 cm and 90 cm above ground level. The manufacturers' instructions for each device were followed, and the same sensor positions were followed during the measurement. In the case of a regular cross-section (cross-sections no. 1_1/2, 2_2), sensors were placed at regular intervals around the circumference.

In the case of irregular cross-sections (cross-sections no. 2_1, 3_1/2), the geometry was determined by the triangulation method using the PiCUS® and ARBOSONIC® devices. The cross-section was split into many triangles (according to the sensors' position), and the lengths of the triangle sides were measured with an electronic calliper from Argus Electronic.

The ARBOTOM® device enables placing of sensors at any point on the circumference. At the point protruding from the basic circle, it is necessary to manually enter the 'correction diameter', which is positive for a convex shape and negative for a concave shape.

There were 12 sensors used for cross-sections no. 1_1, 2_1 and 3_1. For cross-sections no. 1_2, 2_2 and 3_2, 10 sensors were used due to the small diameters and minimum allowed distance between sensors. The position of the first sensor in the chain was oriented towards the north. Sensor positions were marked for subsequent laboratory processing.

Laboratory Measurement

Sound velocity measurement

Cross-sections from tree no. 1 were used for the subsequent processing. During the first phase, the theoretical paths of measured stress waves were drawn on the cross-sections according to the sensors' position (Fig. 2a). The paths were used to determine the intersection points of the signals (10 points were selected and labelled, Fig. 2a). The cross-sections were then cut into six sections with a band saw (Fig. 2b, A-E). Due to the limited capacity of the band saw, sample C had to be divided into two parts (C1 and C2). Processing of the cross-sections into sections minimised the possibility of deviation of the stress wave from the direct (straight) trajectory between the two used sensors (Fig. 2c).

Sound velocities for the radial (v_r) and tangential (v_t) direction of both cross-sections were calculated from STTs according to Eq. 1,

$$C_T = S/\Delta t \quad (1)$$

where C_T is the stress wave velocity (m/s), S is the distance between the two sensors (m), and Δt is the stress wave transition time.

The STT in the radial direction was measured for each section (A-E). The STT in the tangential direction was measured for nine selected intersection points (in the case of C1 and C2, it was not possible to measure the STT of the intersection point closer to the centre due to the insufficient distance between sensors). Distances between sensors were measured using a slide gauge and the STTs of stress wave propagation were measured using the Microsecond Timer® (Fakopp Enterprise Bt., H-9423 Agfalva). In addition, v_t was calculated for each specific intersection point; therefore, these values could be used to determine the statistical correlation between sound velocities, density, and moisture content.

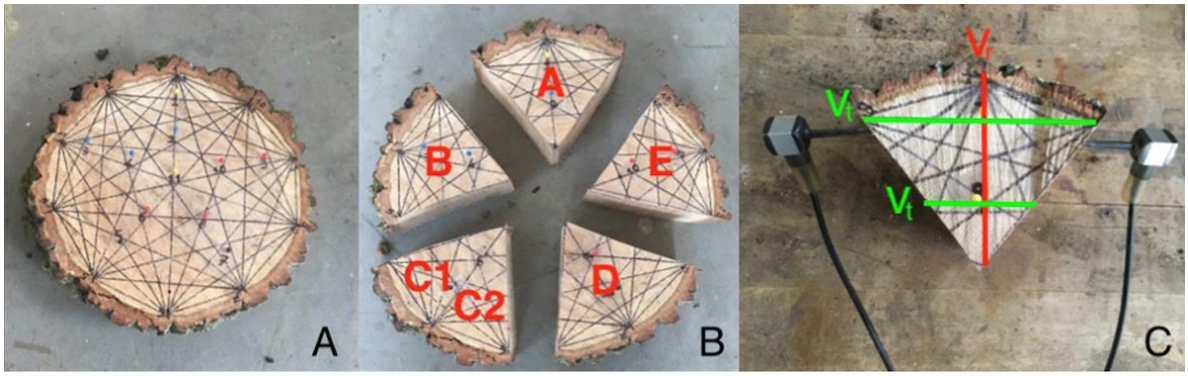

Fig. 2. Experimental set-up: representation of theoretical propagation of acoustic waves (velocity webs) on the disks according to the position of the sensors and the selection of theoretical intersection points of different signals evenly distributed all over the surface areas of discs (A), division of the discs into several sections (B), and measurement of v_r and v_t in proximity to intersection points (C)

Density (ρ) measurement

To measure the wood density (ρ) close to the intersection points, the sections were divided into 18 samples, one for each point where the sound velocity was measured. Density was measured on green wood by the xylometric method.

Moisture content (MC) measurement

All moisture content information (MC) was evaluated by the gravimetric method. Samples were completely dried (MC = 0%) in a kiln SANYO MOV-212P (Sanyo Electric Co., Ltd., Moriguchi, Japan) for 3 days at 103 °C and then weighed. The absolute moisture content was calculated as the weight difference between the fresh and the dried state. Moisture content was expressed as a percentage (%).

Data Analysis

Velocity data were statistically compared using MATLAB 2020a (The MathWorks, Inc., Natick, Massachusetts) and STATISTICA 12 (StatSoft Europe GmbH, Hamburg, Germany) software. Based on the relatively small amount of data and the results of the Shapiro-Wilk test (to verify the normality of the measured data sets), a non-parametric Kruskal-Wallis test was chosen. The comparison of statistical data was divided into three main steps:

1) mutual comparison of sound velocities of individual tomographs on each cross-section
2) mutual comparison of sound velocities of individual tomographs and laboratory measurements of tree no. 1
3) correlation of laboratory-evaluated tangential sound velocities, ρ and MC.

Considering the natural variability of acoustic properties caused by wood orthotropy, it was necessary to select only clear tangential and radial direction velocities from each AT output matrix of velocities (Fig. 3). For the statistical evaluation, two groups of velocities were defined: radial (v_r) and tangential (v_t).

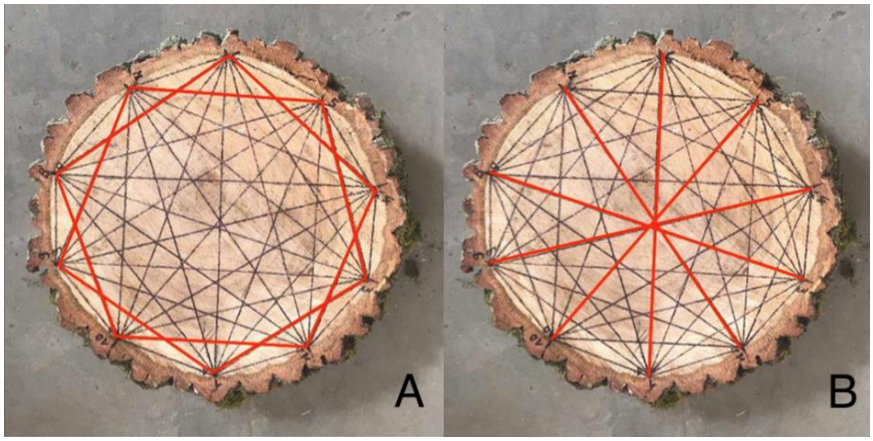

Fig. 3. Graphic representation of the measured tangential (A) and radial (B) stress wave velocities chosen for statistical comparison

To compare the *in situ* assessed sound velocities with those measured in the laboratory, each velocity measured in the laboratory (both radial and tangential) was assigned to corresponding AT velocities of the cross-section. To determine the correlation between tangential sound velocity (v), wood density (ρ) and wood moisture content (MC), a Spearman rank-order correlation test was used. Image reconstructions exported from tomographs and photographs of actual cross-section states were then compared visually.

RESULTS AND DISCUSSION

Comparison of Velocities Measured by All AT Devices

According to the results of the Kruskal-Wallis tests, a statistically significant difference was found among the velocities of each cross-section in both the radial and tangential directions ($p < 0.0001$). According to following multiple comparison tests, a significant difference between velocities measured using PiCUS® and other two devices (ArborSonic® and ARBOTOM®) was proven ($p < 0.05$) for all cross-sections and both directions.

An evident difference between radial and tangential sound velocities (v_r higher than v_t) was demonstrated for all the cross-sections and devices with the exception of velocities measured using ARBOTOM® in cross-section 3_1 (Fig. 4). The difference between measured velocities supports the relation proposed by Palma *et al.* (2018), where tangential velocities in the peripheral area of the measured cross-sections were approximately 70% of the radial ones.

In all the cross-sections, ArborSonic® had the lowest variance between measured velocities in both the radial and tangential directions. In the case of defective cross-sections 2_1 and 3_1, differences between v_r and v_t were attenuated. This was probably caused by the presence of defects, which causes mitigation of the orthotropicity of acoustic properties of wood (McGovem *et al.* 2013).

Although in the case of ArborSonic® and PiCUS® the geometry was obtained by the same procedure, the results of ArborSonic and ARBOTOM® were closer to each other. In the defective cross-sections, higher variability of measured $v_{r,t}$ was demonstrated. Values measured with the acoustic tomograph PiCUS® were lower than those obtained from the

other devices. This significant difference applies to both intact and defective cross-sections. Since the difference cannot be affected by geometry (the same input geometry data for PiCUS® and ArborSonic®), it is probably caused by the hardware used.

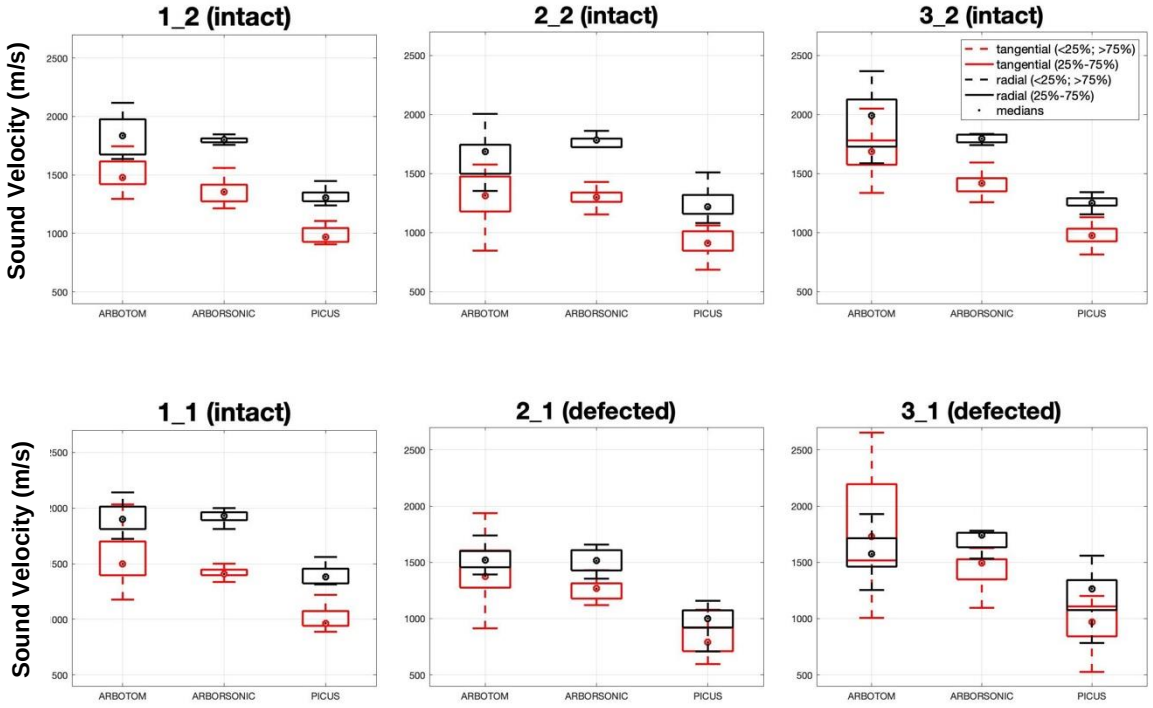

Fig. 4. Radial (v_r) and tangential (v_t) velocities of sections measured by ARBOTOM®, ArborSonic®, and PiCUS® on each cross-section

Table 2. Coefficients of Variation (CV) for Measured Velocities of Each Device on Each Cross-section

Device / Section	**Arbotom®**	**Arborsonic®**	**Picus®**
1_1	12 %	11 %	18 %
1_2	15 %	11 %	13 %
2_1	18 %	11 %	15 %
2_2	18 %	13 %	16 %
3_1	23 %	11 %	28 %
3_2	16 %	11 %	12 %

According to coefficients of variation of measured velocities (Tab. 2), ArborSonic® had the lowest variability of measured data on each cross-section. The variability of measured velocities corresponds to the presence of defects in the measured cross-sections. Higher coefficients of variation of assessed cross-sections can be generally caused by the natural variability of wood and different velocities in different directions (Bucur 2003) rather than device settings.

Comparison of Measured Velocities on Tree No. 1 and Laboratory Assessment

In the case of intact cross-sections of tree no. 1, the highest values (tangential and radial, 2033 m/s and 2141 m/s, respectively) were measured using ARBOTOM®, while the lowest velocities were provided by PiCUS® (888 m/s and 954 m/s) (Fig. 5). Almost all the median velocities measured using ARBOTOM® (v_t = 1490 m/s, v_r = 1880), ArborSonic® (v_t = 1402 m/s, v_r = 1852), and PiCUS® (v_t = 967 m/s, v_r = 1338) were within the range presented by Divos and Divos (2005) (1000 to 2000 m/s).

The smallest variance between the radial and tangential velocities was measured using Microsecond Timer®. Considering the influence of annual curvature of the rings on stress wave propagation (Bucur 2006), the smaller sample size used for laboratory investigation can attenuate this effect, causing lower distinction between directions. In addition, the velocities measured using PiCUS® were not statistically different from those measured in the laboratory using Microsecond Timer® (LAB) for tree no. 1 (Fig. 5).

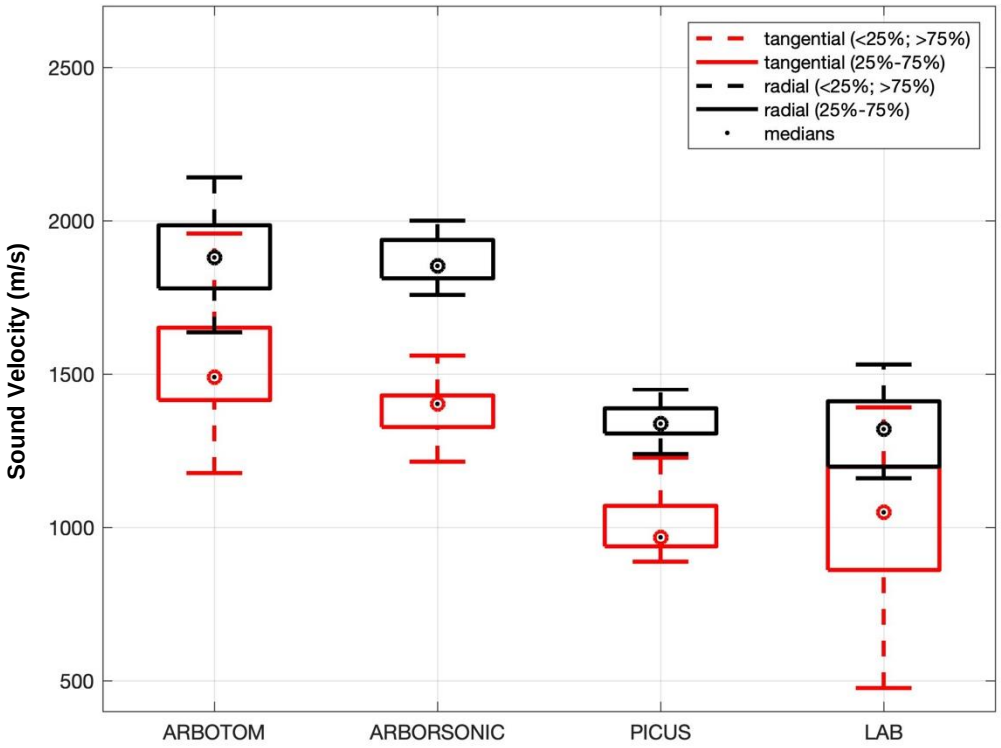

Fig. 5. Radial (v_r) and tangential (v_t) velocities measured by ARBOTOM®, ArborSonic® and PiCUS® in-situ and Microsecond Timer® in the laboratory (LAB) on intact cross-sections from tree no.1

Relationship between Tangential Sound Velocity (v_t), Density (ρ) and Moisture Content (MC)

A moderate positive correlation (R_s = 0.596) between v_t and MC (MC_{avg} = 70%, MC_{CV} = 13%) was found. These data coincide with those of Montero *et al.* (2015), who reported a strong correlation (R_s = 0.98) between longitudinal sound velocity propagation and moisture content. In the case of the density, weak negative correlation (R_s = −0.306)

was established between v_t and ρ (ρ_{avg} = 1675 kg/m^3, ρ_{CV} = 3%). Although the negative correlation corresponds with the theory proposed by Bucur and Chivers (1991), the weak values suggest that no significant correlation between density and moisture content was found.

Comparison of Image Reconstructions (Tomograms)

For reconstruction of the geometry of the intact cross-section 2_1 (Fig. 6), a regular circular shape model was chosen. Therefore, shapes created in tomograms are similar to those for ARBOTOM®. There was a difference in a slightly wavy perimeter made by ARBOTOM®, which was caused by the use of a different system for reconstruction of the geometry.

The small defect marked within the red ellipse (Fig. 6) was not detected by any acoustic tomograph. These results align with those of Gilbert and Smiley (2004) and Rabe *et al.* (2004), who state that the average resolution for acoustic tomographs is between 5 cm and 10 cm, and therefore small defects are not usually detected. Lighter peripheric zones in the image reconstruction of the PiCUS® tomograph (Fig. 6C) are described by Argus Electronic (2017) as lower tangential velocities in the cross-section periphery altering the image reconstruction.

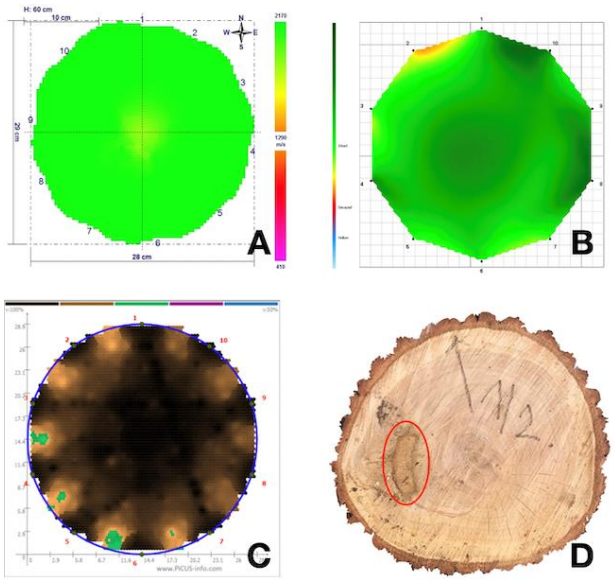

Fig. 6. Reconstructions of images (tomograms), ARBOTOM® (A), ArborSonic® (B), PiCUS® (C), and the assessed mostly intact cross-section 1_2

For reconstruction of the geometry of the defective cross-section 2_1 (Figure 7), the irregular geometry model was chosen. For PiCUS® and ArborSonic®, the geometry was recorded using a triangulation method. Therefore, reconstructions of the geometry for both were identical and the created cross-section geometry was relatively precise. In addition, PiCUS® software optimised the irregular shape by automatic curvature of the connecting lines between sensors.

ARBOTOM®'s geometry was modified from the regular shape according to deviations from circularity at each measuring point. This approach did not provide such precise reconstruction of the shape of the cross-section.

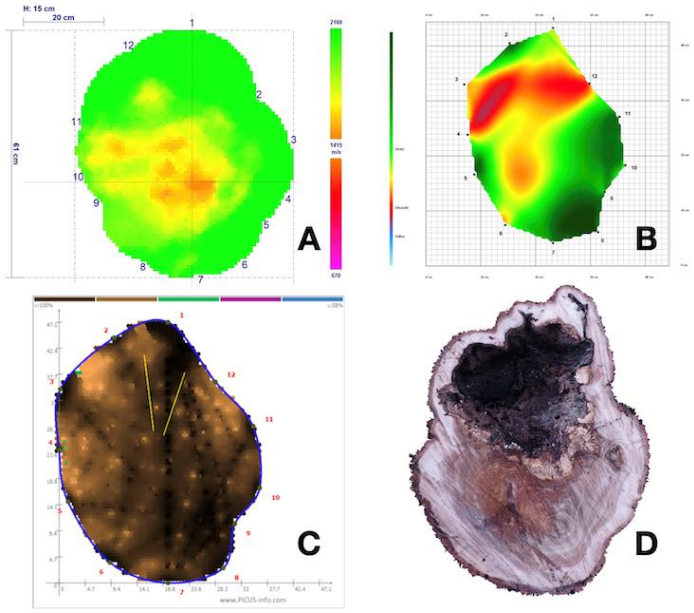

Fig. 7. Reconstructions of images (tomograms), ARBOTOM® (A), ArborSonic® (B), PiCUS® (C), and the assessed defective cross-section 2_1

According to the reconstructions of images (Fig. 7, A-C), a defect was clearly detected by both the ARBOTOM® and ArborSonic® devices (Fig. 7, A, B). However, according to the colour legend used for each tomograph, neither of them showed a hollow section, but only a portion of degraded wood.

In the PiCUS® tomogram, no obvious defect was shown, and there were only a few lighter spots all across the section. AT results could be influenced by the conic shape of the present cavity. The defect ended 10 cm above the measurement level, which could mean that the stress wave signal flowed above the defect in a shorter time. For this reason, the vertical defect distribution should also be considered in the AT assessment.

CONCLUSIONS

1. A statistically significant difference between values measured using the acoustic tomograph PiCUS® and data from two other devices (ARBOTOM® and ArborSonic®) was shown for each measured cross-section. Velocities registered by the PiCUS® acoustic tomograph were significantly lower than values obtained from ARBOTOM® and ArborSonic®.
2. Radial and tangential velocities differed from each other. In data obtained from the defective cross-sections, this difference was attenuated.
3. The variability of measured data did not correspond to the presence of defects in assessed cross-sections.
4. Data measured in the laboratory were most similar to those measured using PiCUS®. There was statistical difference between values measured in the laboratory and those measured using ARBOTOM® and ArborSonic tomographs in both the radial and

tangential directions.

5. Acoustic tomographs designed for assessment of standing trees differed from each other in measured data (mostly PiCUS® from both ARBOTOM® and ArborSonic®) and also image reconstructions. Although no statistically significant difference was found between measured velocities ($v_{r,t}$) of ARBOTOM® and ArborSonic®, their tomograms differed.
6. No strong correlation between sound velocity and density was shown, while a moderate degree of correlation was found between sound velocities and moisture contents.
7. Complex shapes of defects in standing trees (*e.g.* conical shape; Fig. 7) can significantly influence acoustic tomography results due to possible stress wave signal transition above the defect.
8. Correct interpretation of AT measurements should consider the influence of different factors, including the device used.

ACKNOWLEDGMENTS

The work was supported by The Ministry of Education, Youth and Sports of Czech Republic, project ERC CZ no. LL1909 "Tree Dynamics: Understanding of Mechanical Response to Loading".

REFERENCES CITED

Alméras, T., Thibaut, A., and Gril, J. (2005). "Effect of circumferential heterogeneity of wood maturation strain, modulus of elasticity and radial growth on the regulation of stem orientation in trees," *Trees - Structure and Function* 19(4), 457-467. DOI: 10.1007/s00468-005-0407-6

Alves, R. C., Mantilla, J. N. R., Bremer, C. F., and Carrasco, E. V. M. (2015). "Application of acoustic tomography and ultrasonic waves to estimate stiffness constants of muiracatiara brazilian wood," *BioResources* 10(1), 1845-1856. DOI: 10.15376/biores.10.1.1845-1856

Arciniegas, A., Prieto, F., Brancheriau, L., and Lasaygues, P. (2014). "Literature review of acoustic and ultrasonic tomography in standing trees," *Trees - Structure and Function* 28(6), 1559-1567. DOI: 10.1007/s00468-014-1062-6

Argus electronic (2017). *PiCUS Tomograph Manual of PC Software Q74*,(Release 2.17) Argus Electronic gmbh, Rostock, Germany.

Baar, J., Tippner, J., and Gryc, V. (2012). "The influence of wood density on longitudinal wave velocity determined by the ultrasound method in comparison to the resonance longitudinal method," *European Journal of Wood and Wood Products* 70(5), 767-769. DOI: 10.1007/s00107-011-0550-2

Brashaw, B. K., Bucur, V., Divos, F., Gonçalves, R., Lu, J., Meder, R., Pellerin, R. F., Potter, S., Ross, R. J., Wang, X., and Yin, Y. (2009). "Nondestructive testing and evaluation of wood: A worldwide research update," *Forest Products Journal* 59(3), 7–14.

Bucur, V. (2003). *Springer Series in Wood Science: Nondestructive Characterization and*

Imaging of Wood, Springer Berlin Heidelberg.
Bucur, V. (2006). *Acoustics of Wood*, Springer Berlin Heidelberg.
Bucur, V., and Chivers, R. (1991). "Acoustic properties and anisotropy of some Australian wood species," *Acta Acustica united with Acustica* 75, 69-74(6).
Burcham, D. C., Brazee, N. J., Marra, R. E., and Kane, B. (2019). "Can sonic tomography predict loss in load-bearing capacity for trees with internal defects? A comparison of sonic tomograms with destructive measurements," *Trees - Structure and Function*, 1–35. DOI: 10.1007/s00468-018-01808-z
Divos, F., and Divos, P. (2005). "Resolution of stress wave based acoustic tomography," in: *14th International Symposium on Nondestructive Testing of Wood*, Shaker Verlag, Eberswalde, Germany.
Du, X., Li, J., Feng, H., and Chen, S. (2018). "Image reconstruction of internal defects in wood based on segmented propagation rays of stress waves," *Applied Sciences (Switzerland)* 8(10). DOI: 10.3390/app8101778
Espinosa, L., Arciniegas, A., Cortes, Y., Prieto, F., and Brancheriau, L. (2017). "Automatic segmentation of acoustic tomography images for the measurement of wood decay," *Wood Science and Technology*, 51(1), 69-84. DOI: 10.1007/s00226-016-0878-1
Gilbert, E. A., and Smiley, E. T. (2004). "Picus sonic tomography for the quantification of decay in white oak (*Quercus alba*) and hickory (*Carya* spp.)," *Journal of Arboriculture* 30(5), 277-280.
Ilic, J. (2003). "Dynamic MOE of 55 species using small wood beams," *Holz als Roh - und Werkstoff* 61(3), 167-172. DOI: 10.1007/s00107-003-0367-8
Kumar, A., Pathak, P. P., and Dass, N. (2016). "A study of speed of sound in water," *IOSR Journal of Applied Physics* 08(04), 21-23. DOI: 10.9790/4861-0804022123
Liang, S., Wang, X., Wiedenbeck, J., Cai, Z., and Fu, F. (2008). "Evaluation of acoustic tomography for tree decay detection," in: *15th International Symposium on Nondestructive Testing of Wood*, 49-54.
Maurer, H., Schubert, S. I., Bächle, F., Clauss, S., Gsell, D., Dual, J., and Niemz, P. (2006). "A simple anisotropy correction procedure for acoustic wood tomography," *Holzforschung* 60(5), 567-573. DOI: 10.1515/HF.2006.094
McGovem, M., Senalik, A., Chen, G., Beall, F. C., and Reis, H. (2013). "Effect of decay on ultrasonic velocity and attenuation measurements in wood," *Materials Evaluation* (217), 1217-1231.
Montero, M. J., de La Mata, J., Esteban, M., and Hermoso, E. (2015). "Influence of moisture content on the wave velocity to estimate the mechanical properties of large cross-section pieces for structural use of scots pine from Spain," *Maderas: Ciencia y Tecnologia* 17(2), 407-420. DOI: 10.4067/S0718-221X2015005000038
de Oliveira, F. G. R., and Sales, A. (2006). "Relationship between density and ultrasonic velocity in Brazilian tropical woods," *Bioresource Technology* 97(18), 2443-2446. DOI: 10.1016/j.biortech.2005.04.050
Ordóñez-Barona, C., Sabetski, V., Millward, A. A., Urban, J., Steenberg, J., and Grant, A. (2018). "The influence of abiotic factors on street tree condition and mortality in a commercial-retail streetscape," *Arboriculture & Urban Forestry* 44(3), 133-144.
Palma, S. S. A., Gonçalves, R., Trinca, A. J., Costa, C. P., Reis, M. N., and Martins, G. A. (2018). "Interference from knots, wave propagation direction, and effect of juvenile and reaction wood on velocities in ultrasound tomography," *BioResources* 13(2), 2834-2845. DOI: 10.15376/biores.13.2.2834-2845

Rabe, C., Ferner, D., Fink, S., and Schwarze, F. W. M. R. (2004). "Detection of decay in trees with stress waves and interpretation of acoustic tomograms," *Arboricultural Journal* 28(1–2), 3-19. DOI: 10.1080/03071375.2004.9747399

Rioux, D. (2004). "A non-invasive acoustic tool revealing decay in trees," *Phytoprotection* 85(2),68.

Sandoz, J. L. (1989). "Grading of construction timeber by ultrasound," *Wood Science and Technology* 23(1), 95-108. DOI: 10.1007/BF00350611

Schubert, S. (2007). *Acousto-Ultrasound Assessment of Inner Wood-Decay in Standing Trees: Possibilities and Limitation*s, Ph.D. Dissertation, Swiss Federal Institute of Technology Zurich, Switzerland.

Siegert, B. (2013). "Comparative analysis of tools and methods for the evaluation of tree stability," *Arborist News* 22(2), 26-31.

Sterken, P. (2005). *A Guide For Tree-Stability Analysis*, Asociación Española de Arboricultura, Valencia, Spain.

Tomikawa, Y., Iwase, Y., Arita, K., and Yamada, H. (1986). "Nondestructive inspection of a wooden pole using ultrasonic computed tomography," *IEEE Transactions on Ultrasonics, Ferroelectrics, and Frequency Control* 33(4), 354-358. DOI: 10.1109/T-UFFC.1986.26842

Unterwieser, H., and Schickhofer, G. (2011). "Influence of moisture content of wood on sound velocity and dynamic MOE of natural frequency- and ultrasonic runtime measurement," *European Journal of Wood and Wood Products* 69(2), 171-181. DOI: 10.1007/s00107-010-0417-y

Wang, X. (2013). "Acoustic measurements on trees and logs: A review and analysis," *Wood Science and Technology* 47(5), 965-975. DOI: 10.1007/s00226-013-0552-9

Wang, X. P., Divos, F., Pilon, C., Brashaw, B. K., Ross, R. J., and Pellerin, R. F. (2004). *Assessment of Decay in Standing Timber using Stress Wave Timing Nondestructive Evaluation Tools - A Guide for Use and Interpretation* (Report No. PL-GTR-147), U.S. Department of Agriculture, Forest Products Laboratory, Madison, WI.

Wang, X., Ross, R. J., McClellan, M., Barbour, R. J., Erickson, J. R., Forsman, J. W., and McGinnis, G. D. (2001). "Nondestructive evaluation of standing trees with a stress wave method," *Wood and Fiber Science* 33(4), 522-533.

Wen, J., Gao, L., Xiao, X., Xiao, Z., and Li, C. (2016). "Detection and measurement of internal defects for tree trunk by GPR," *International Journal of Simulation: Systems, Science and Technology*, 17(31), 9.1-9.6. DOI: 10.5013/IJSSST.a.17.31.09

Article submitted: November 27, 2020; Peer review completed: February 6, 2021;
Revised version received and accepted: March 3, 2021; Published: March 5, 2021.
DOI: 10.15376/biores.16.2.3046-3058